ISSN 0018-1439, High Energy Chemistry, 2015, Vol. 49, No. 6, pp. 438–448. © Pleiades Publishing, Ltd., 2015.

LASER CHEMISTRY

Effect of Laser Fluence on the Characteristics of CdSe Nanoparticles Prepared by Laser Ablation in Methanol[1]

R. A. Ismail[a], N. F. Habubi[b], and A. N. Abd[c]

[a] *Department of Applied Sciences, University of Technology Baghdad, Iraq*
e-mail: raidismail@yahoo.com

[b] *Physics Department, Education Faculty, University of Al-Mustansiriyah Baghdad, Iraq*

[c] *Physics Department, Science Faculty, University of Al-Mustansiriyah Baghdad, Iraq*

Received Jnuary 11, 2015; in final form, May 05, 2015

Abstract—The effect of laser fluence on structural, morphological, optical, and electrical properties of CdSe nanoparticles NPs prepared by irradiating a CdSe target, immersed in methanol, with Nd:YAG laser pulses at laser fluences in the range of (1.32–2.92) J/cm^2 has been studied. X-ray diffraction XRD measurements disclosed that the CdSe NPs were of wurtzite hexagonal crystal structure. Transmission electron microscopy investigation revealed that the synthesized CdSe particles are spherical and have an average particle size in the range of (37–94 nm). Scanning electron microscope SEM and transmission electron microscope TEM investigations showed that the shape and size of the synthesized CdSe NPs depend on laser fluence. The nanoparticles distribution was correlated with laser fluence. Atomic force Microscopic AFM investigations showed highly dispersed ball-shape CdSe particles. The optical energy gap of CdSe nanoparticles prepared has been determined from optical properties and found to be in the range of (1.7–2.05 eV). Optical constants of CdSe NPs were determined from transmittance and reflectance spectra. Hall measurement showed that the CdSe nanoparticles were n-type and their carrier concentration and mobility was investigated.

Keywords: laser ablation, nanoparticles, colloidal, cadmium selenide, optical properties, laser fluence

DOI: 10.1134/S0018143915060089

Cadmium selenide (CdSe) is an important semiconducting material due to its potential use in photoconductive devices and solar cells [1–4]. CdSe thin films have widely been studied because of its high absorption coefficient and nearly optimum band gap energy (1.73 eV). It finds a wide range of applications in low cost devices such as light emitting diodes, solar cells, photodetectors, electro photography and laser diodes [1, 4–6]. Cadmium selenide nanoparticles have different optical and electrical properties compared to bulk CdSe due to the strong confinement of excited electrons and holes [7]. The band gap of CdSe colloidal nanoparticles can be tuned through the control of nanoparticles size to give emission from red to blue [8]. These superior properties made CdSe NPs useful for optoelectronic devices, high efficiency solar cells, nano-sensors, and biomedical applications [9]. Many methods are adapted to synthesis CdSe NPs such as chemical precipitation, chemical bath deposition CBD, surfactant assisted hydrothermal, electrochemical, laser ablation etc. [10]. Laser ablation in liquid is a very interesting technique due to simplicity, high purity and stability of colloids, doesn't need catalyst or vacuum, good control on particles size, and safe handling of colloids [11]. Up to best of our knowledge, few data have been published related to the laser ablation of CdSe NPs in liquid [1, 12, 13]. Recently, Sabit et al. [14] investigated the photovoltaic characteristics of CdSe quantum dots prepared by pulsed frequency quadrupled Nd:YAG laser in methanol. Recently we have reported that liquid type affects the properties of colloidal CdSe nanoparticles synthesized by laser ablation [15]. In this paper, we report on the effect of laser fluence on the structural, optical and electrical properties of CdSe NPs synthesised by laser ablation in methanol.

EXPERIMENTAL DETAILS

The laser used for the ablation is Nd:YAG operating at 10 Hz repetition rate, with 7 ns pulse width and wavelength of 1064 nm. The laser pulses were focused by a 20 cm positive lens onto a cleaned 2 mm thick CdSe bulk sample (99.99% purity provided from Poch company) immersed in methanol at various laser fluences (1.32, 1.76, 2.12, 2.51 and 2.92 J/cm^2) with an ablation time of 20 min. The energy of laser pulse was measured using calibrated Joule meter after taking in-

[1] The article is published in the original.

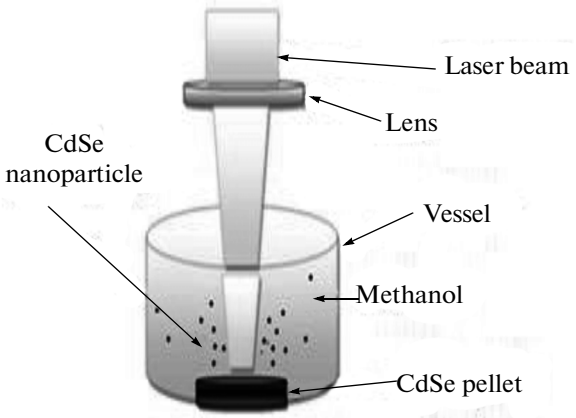

Fig. 1. Schematic diagram of laser ablation system.

to account the effect methanol transmittance. The CdSe target is placed in the bottom of a quartz vessel filed with 20 mL of methanol, see Figure 1. X-ray diffractometer (XRD-6000, Shimadzu, X-ray, diffractometer) with Cuka radiation at a wavelength of (l = 0.154056 nm) was utilized to investigate the structural properties of CdSe NPs deposited on glass substrate. The optical absorption of colloidal CdSe NPs was measured using a spectrophotometer (Cary, 100 Conc plus, UV-Vis-NIR, Split- beam Optics, Dual detectors) in the range of (200–900) nm. The shape and size of the CdSe nanoparticles were investigated by using TEM (type CM10 pw 6020, Philips—Germany) after depositing some drops of CdSe onto a carbon coated copper grid. The morphology of the CdSe NPs was investigated by using SEM (FE-SEM Image Library) and AFM (AA 3000 Scanning Probe Microscope). The electrical characterization was carried out using Hall measurements after making ohmic contacts on the CdSe NPs film deposited on glass substrate by depositing of Al thick film through special mask. The thickness of the films was measured using ellipsometer (Angstrom sun Technologies Ins). All above measurements were carried out at room temperature.

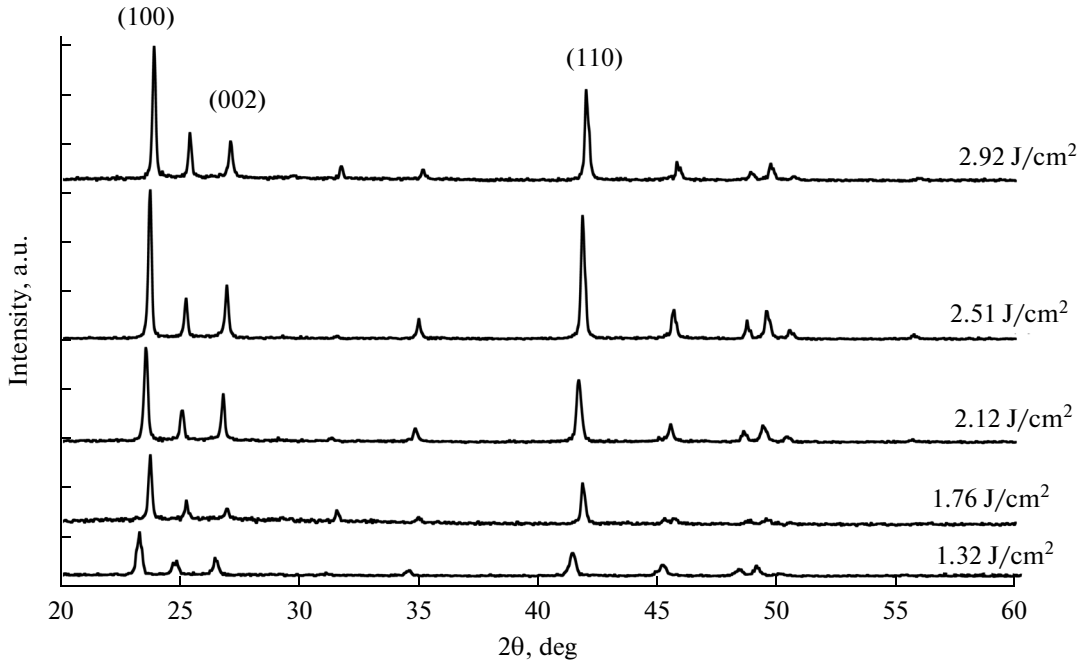

Fig. 2. XRD patterns of CdSe nanoparticles synthesized at various laser fluencies.

Table 1. XRD data of CdSe nanoparticles ablated at different laser fluences

Laser fluence (J/cm^2)	2θ (deg)	*hkl* Plane	*d* observed (Å)	*d* ASTM (Å)	FWHM (deg)	*D* (nm)	$\delta \times 10^{14}$ $lin.m^{-2}$	$\eta \times 10^{-4}$ $lin^{-2}.m^{-4}$
1.32	23.32	(100)	3.81	3.79	0.27	31.21	10.26	11.59
	26.51	(002)	3.35	3.34	0.25	–	9.04	10.88
	41.44	(110)	2.17	2.16	0.284	–	10.34	11.64
1.76	23.6	(100)	3.76	3.74	0.18	46.84	4.55	7.72
	26.82	(002)	3.32	3.30	0.16	–	3.82	7.08
	41.70	(110)	2.16	2.15	0.20	–	5.38	8.39
2.12	23.77	(100)	3.78	3.72	0.18	46.34	4.65	7.80
	25.29	(002)	3.51	3.50	0.15	–	3.35	6.63
	41.88	(110)	2.15	2.14	0.16	–	3.52	6.79
2.52	23.76	(100)	3.74	3.72	0.16	50.20	3.96	7.20
	26.98	(002)	3.3	3.28	0.16	–	3.73	6.99
	41.87	(110)	2.15	2.14	0.16	–	3.27	6.54
2.92	23.94	(100)	3.71	3.69	0.16	52.72	3.59	6.86
	25.44	(002)	3.49	3.48	0.16	–	3.57	6.84
	42.03	(110)	2.14	2.13	0.15	–	3.15	6.42

RESULTS AND DISCUSSION

Structural Properties

The X-ray diffraction spectra of CdSe nanoparticles films prepared at different laser fluences are given in Fig. 2. XRD spectra showed that all the synthesized CdSe NPs are of hexagonal (Wurtzite) structure according to JCPDS file No: 77-2307 [16]. The observed and standard of "d" values of CdSe NPs prepared at low laser fluences is shown in table 1, with a slight change of "d" values noticed at higher laser fluences. A shift in the diffracted peaks related to (100 and 110) planes was observed as laser fluence increases due to structural defects and stresses. The intensity and the value of full width at half maximum FWHM of main diffraction peaks increased with laser fluence, indicating the formation of smaller particles. No diffraction peaks related to other phases were observed in the XRD spectra of CdSe NPs. The mean crystallites size D of (111 plane was determined using the following Debye–Scherrer formula (XRD line broadening) [17] and listed in Table 1.

$$D = \frac{0.9\lambda}{\beta \cos\theta} \ldots\ldots\ldots, \quad (1)$$

where λ is the wavelength of x-ray, θ is the diffraction angle and β is the FWHM. Increasing of laser fluence from 1.3 to 2.9 J/cm^2 has led to an increase in the crystal size from 31 to 53 nm. From analysis, the average grain size of CdSe particles was between (31 to 56 nm). The strong and narrow peaks may be ascribed to the preferential growth along (100, 110) planes of CdSe

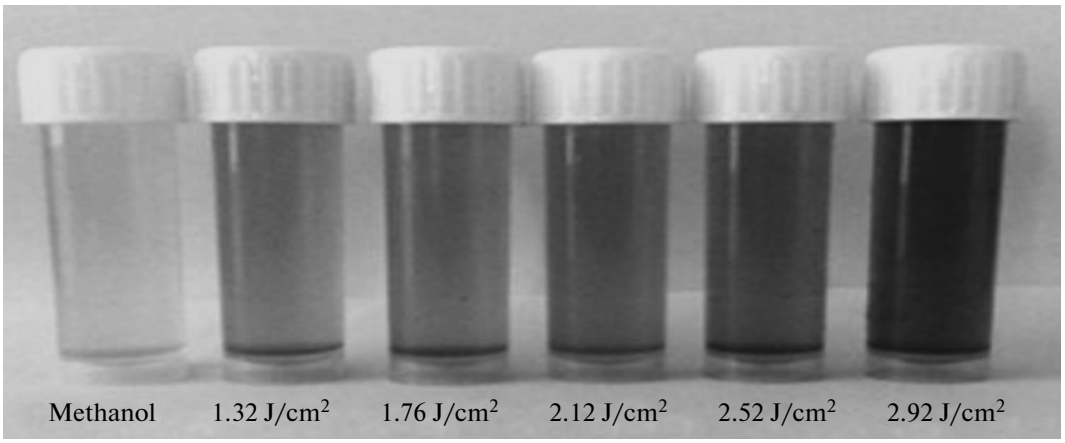

Fig. 3. Fresh colloidal suspensions of CdSe prepared at different laser fluencies.

crystallites. The strain (η) and the dislocation density (δ) were evaluated by using the following relations [18] and the results indicated their decrease with increasing grain size, see Table 1:

$$\eta = \frac{\beta \cos\theta}{4}, \quad (2)$$

$$\delta = \frac{1}{D^2}. \quad (3)$$

Optical Properties of the Crystalline CdSe Thin Film

The color of fresh CdSe colloidal suspension has found to be depended on the laser fluence, for CdSe NPs synthesized at low laser fluence was brown and changed to dark gray when the laser fluence increased as clearly shown in Fig. 3, this result was probably due to the variation of CdSe particle size and concentration with laser fluence.

Fig. 4 shows the absorption spectra of CdSe NPs. The absorption characteristics are a useful tool to analyze nanomaterials. It is clearly seen from this figure that the absorption decreases sharply below ~400 nm. Besides, remarkable variations in the absorption spectra within the range 500–600 nm were noticed due to the fact that the individual crystallites may have the dimensions of the field "size effect" [19]. Decreasing of optical absorption with increasing laser fluence is due to scattering effect resulted from formation of large particles at high laser fluence [20].Using Tauc relationship, the absorption data can help estimating the energy band gap of CdSe by plotting the square of $(\alpha h\nu)$ versus $(h\nu)$. The extrapolation of the straight line to $(\alpha h\nu)^2 = 0$ gives the value of energy gap as shown in Fig. 5. The values of band gap of CdSe NPs were within the range 1.75–2.25 eV depending on laser fluence values. The transition of electrons was direct. The band gap decrease with increasing the laser fluence is attributed to the formation of agglomerated CdSe particles. The large value of band gap of CdSe (blue shift) prepared at lower laser fluence (1.32 J/cm^2) as compared to its value for bulk (1.7 eV) has resulted from nanosized effect [21]. The variation of refractive

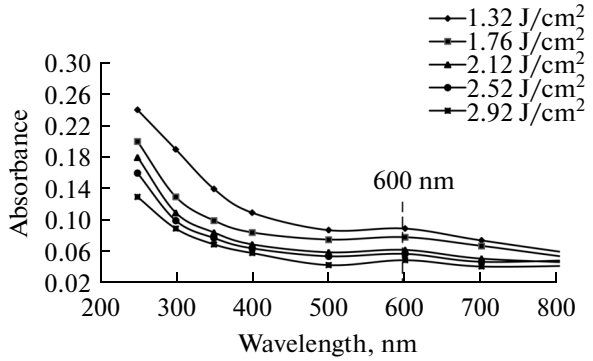

Fig. 4. Optical Absorbance spectra of colloidal CdSe nanoparticles.

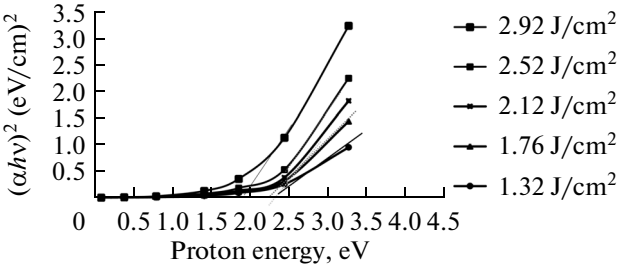

Fig. 5. $(\alpha h\nu)^2$ versus photon energy plot of CdSe NPs prepared at different laser fluencies.

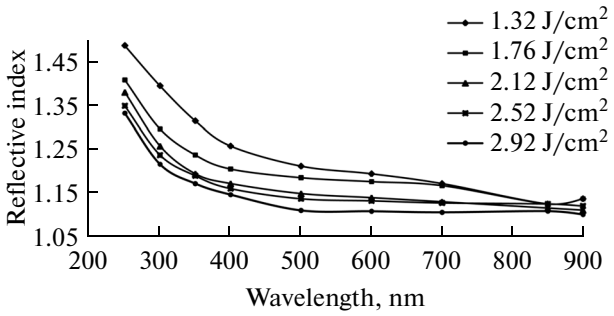

Fig. 6. Refractive index as function of wavelength.

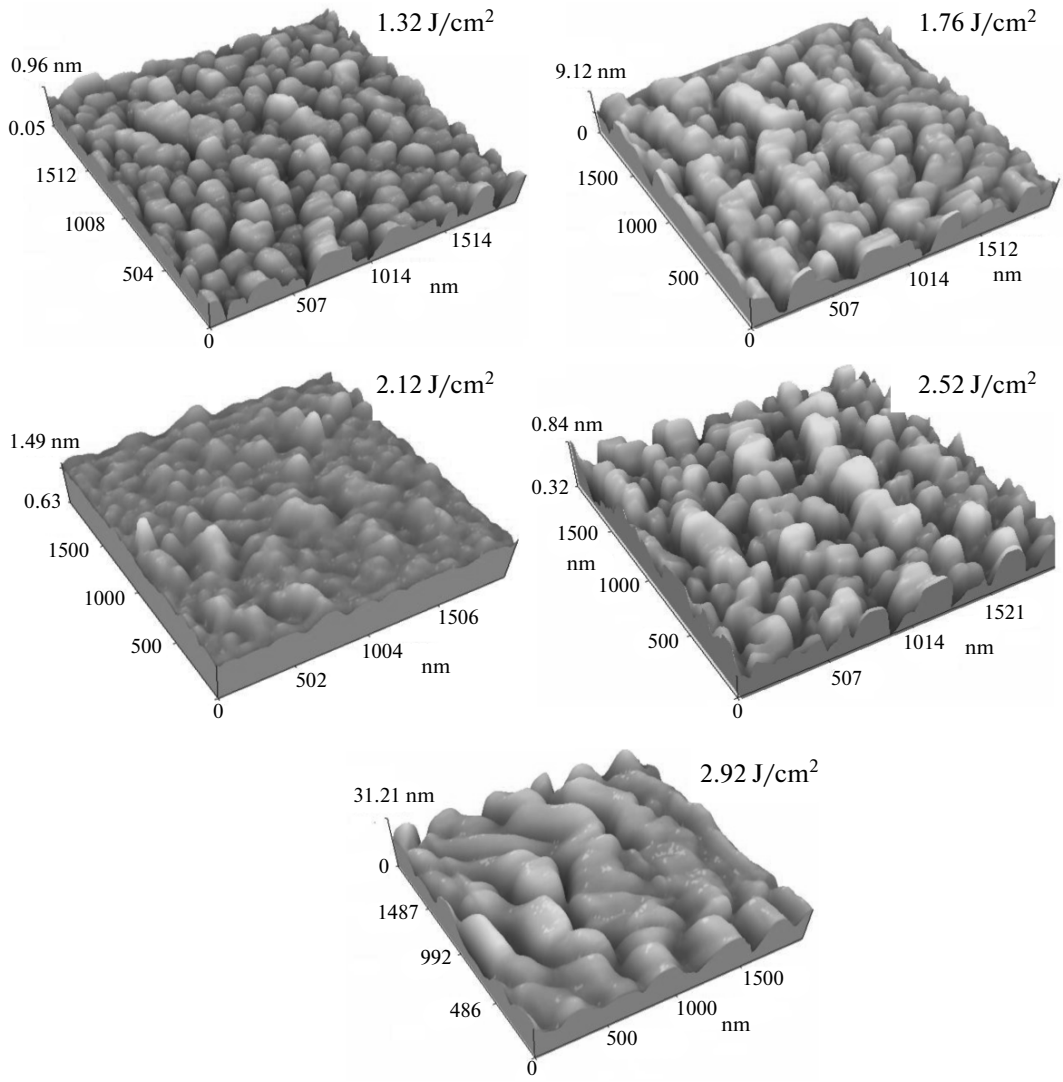

Fig. 7. 3D AFM images of CdSe nanoparticles synthesized at different laser fluencies.

index versus wavelength plot for CdSe NPs prepared at different laser fluences is given in Fig. 6. It shows clearly a sharp decrease of the refractive index with wavelength up to 400 nm and tends to saturate after ~500 nm. Furthermore, and due to the particle size effect, the refractive index of CdSe NPs was found to decrease at certain wavelengths when increasing the laser fluence.

AFM Studies

AFM images of CdSe NPs synthesized at various laser fluences are shown in Fig. 7. The NPs were highly dispersed ball-shaped and the grains are homogenous and aligned vertically. By using special software, the root mean square RMS value of surface roughness and average grain size were estimated and presented in Table 2. The CdSe NPs prepared at high laser fluence are agglomerated and formed larger particles as shown in Fig. 7e. The average grain size results (listed in Table 2) disagree with those estimated from XRD due to the fact that the AFM measurement directly visualizes the grains regardless of the degree of structural defects, while the estimation of particle size by XRD is based on size of defect free volume [22]. In Table 2, it is clearly seen that the root mean square of surface roughness increases with laser fluence increase. Increasing of laser fluence means delivering of more energy implies ablating large amount of CdSe material [23].

Electrical Measurements

The Hall Effect measurements show that all synthesized nanostructured CdSe films are *n*-type. The mobility and carrier concentration of nanostructured CdSe film are measured as function of laser fluence and depicted in Fig. 8. It is obvious from this figure that the mobility increases abruptly for laser fluences higher than 2.5 J/cm^2 due to the formation of larger CdSe particles size, i.e. the mobility is size-dependent. Beard et al. [24] reported that due to strong confinement, the mobility of CdSe NPs increases as an r^4, where r is the radius of nanoparticles. The maximum value of electron mobility was found to be around 185 cm^2 V^{-1} s^{-1} at 2.9 J/cm^2, which is lower than that of bulk CdSe.

Table 2. RMS of surface roughness and average grain size of CdSe NPs

Laser fluence (J/cm^2)	Grain size (nm)	Root mean square of surface roughness (nm)
1.32	62	0.11
1.76	76	0.14
2.12	84	0.15
2.52	86	1.76
2.92	166	4.49

Surface Morphology

Fig. 9 shows SEM images with two magnifications of CdSe NPs prepared at different laser fluences. In this set of SEM images it can confirmed that these NPs have different morphologies. It was noticed that the morphology of CdSe NPs is not uniform and consists of many small irregular nanoparticles. The SEM images of CdSe NPs synthesized at higher laser fluences shows that the particles are well agglomerated.

The TEM images and particle size distributions of CdSe NPS prepared at different laser fluences are shown in Fig. 10. The TEM images show that the CdSe NPs are well crystallized and are mostly separat-

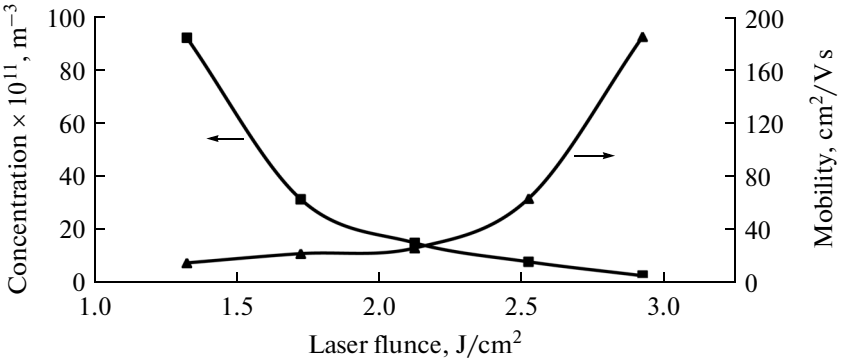

Fig. 8. Carrier concentration and Hall mobility versus laser fluence.

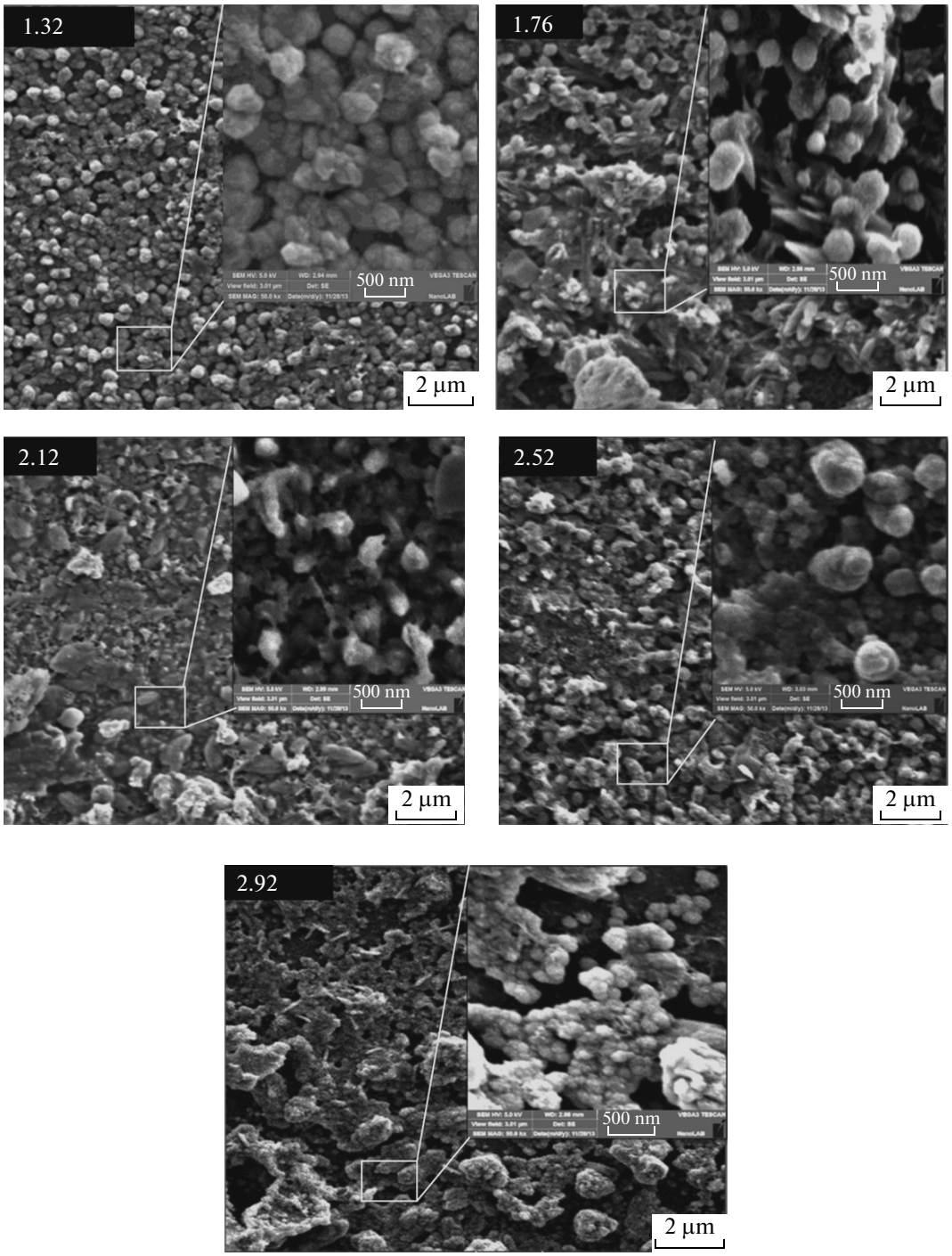

Fig. 9. SEM images of CdSe nanoparticles prepared at different laser fluences. The insets are high magnification SEM images.

ed. The images confirm that the particles have spherical shape and the particle size was in the range of (37–94 nm) depending on laser fluence. The size distributions of these nanoparticles shows a Gaussian profile. The production of different sizes particles at fixed laser fluence can be explained on the basis that the newly formed nanoparticles which lie in the direction of laser radiation will have smaller sizes due to their successive interaction with laser pulses by the inter-pulse absorption process [25]. No significant effect of laser fluence on the shape of synthesized nanoparticles was detected.

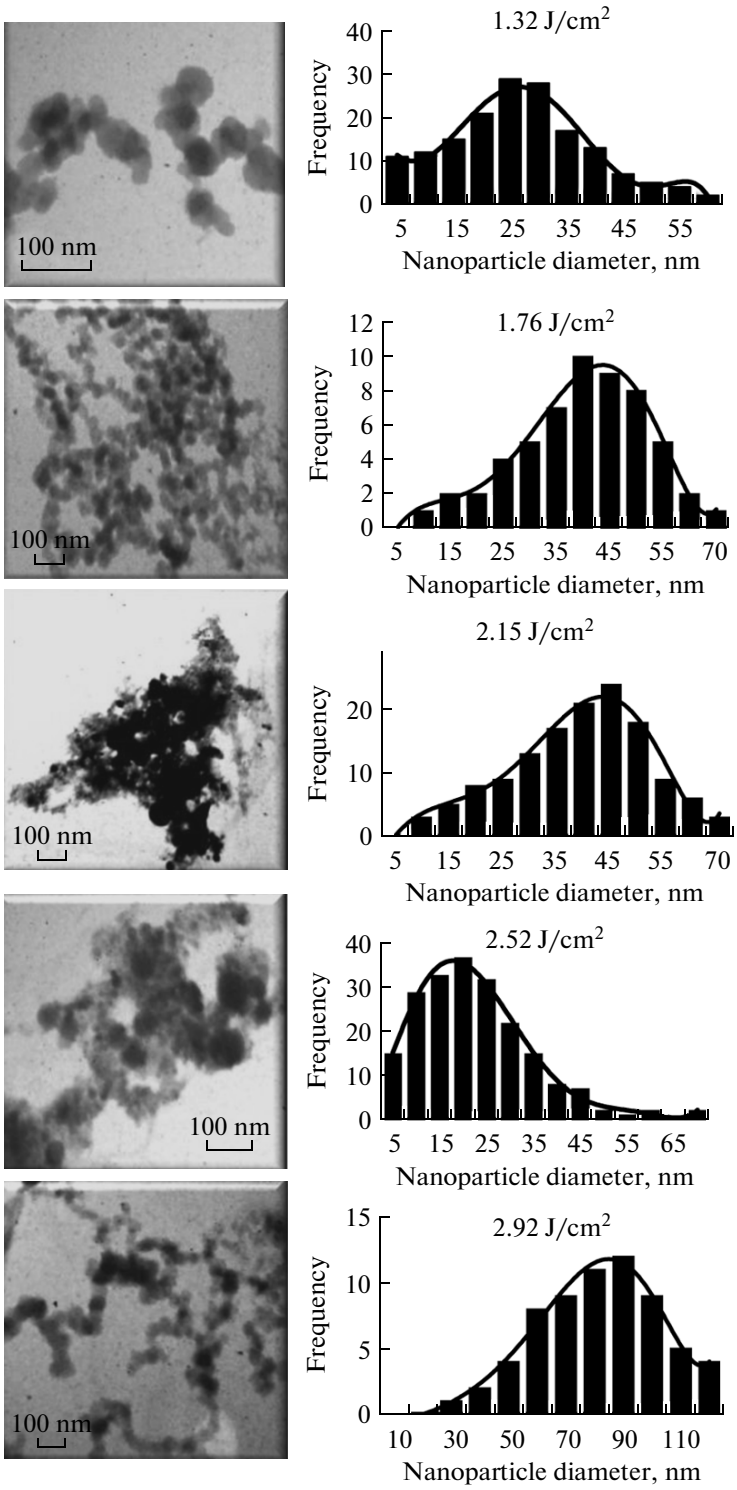

Fig. 10. TEM images of CdSe nanoparticles and their size distribution histograms.

Photoluminescence (PL)

PL emission spectra of CdSe NPs prepared at different laser fluences were recorded at room temperature with excitation source of 480 nm wavelength as shown in Fig. 11. A single sharp broad emission peak centered at the green region ~575 nm (2.15 eV) with FWHM of ~23 nm was observed in the emission spectrum of CdSe NPs synthesized at 1.32 J/cm^2. The PL

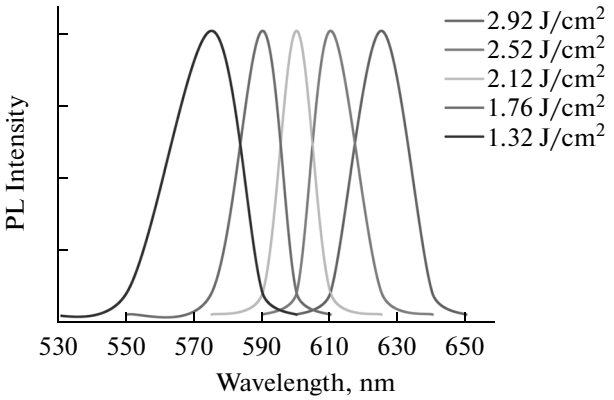

Fig. 11. PL spectra of CdSe nanoparticles.

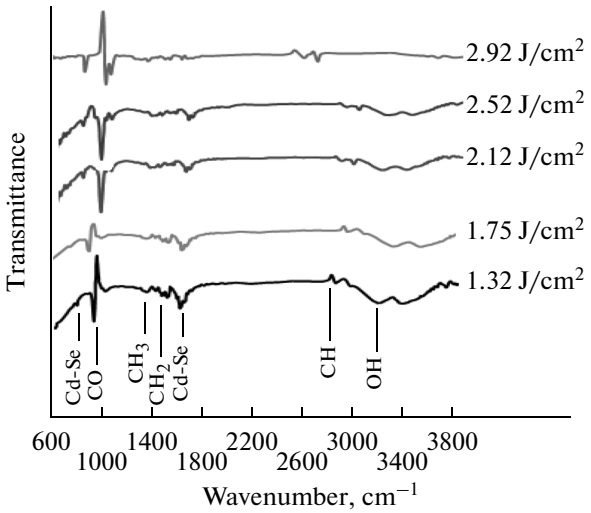

Fig. 12. FT-IR spectra of CdSe nanoparticles.

Table 3. PL Emission wavelength, energy and FWHM of CdSe NPs versus laser

Laser fluence (J/cm^2)	Emission wavelength (nm)	Emission energy (eV)	FWHM (nm)
1.32	575	2.15	23
1.76	590	2.10	14
2.12	600	2.06	12
2.52	610	2.03	14.5
2.92	625	1.98	19

spectra of CdSe NPs prepared at higher laser fluences emit light of different colors. This result can be attributed to the quantum confinement effect and is in good agreement with the results of SEM and TEM. The coloration is directly related to the energy levels of nanoparticles. Table 3 shows the PL emission wavelength and emission energy of CdSe NPs as a function of laser fluence. It is clear from this table that a large tuning can be obtained via variation of the laser fluence. Increasing the laser fluence to 2.92 J/cm^2 caused a red ~625 nm (1.98 eV) shift in the PL peak due to the broad size distribution of nanoparticles. The PL spectra of CdSe NPs show a Gaussian envelope arose from inhomogeneous broadening due to size and shape distribution within QDs and homogeneous broadening due to the thermal energy (26 meV at room temperature) [26]. The observed PL blue shift peaks are in good agreement with optical band gap estimated from the absorption data. No significant change in the intensity of PL emission was noticed after increase of laser fluence.

FT-IR Investigation

The FT-IR spectra (transmittance mode) of CdSe NPs presented in Fig. 12 shows the existence of cadmium selenide compound and methanol solvents. The Cd–Se band stretching is observed at about 722 cm^{-1}. The sharp peak at 1000 nm belongs to the vibration band of CO. All other peaks are corresponding to the structural bond of methanol with cadmium selenide NPs such as ~1377, 1463, 2853, 2924 and 2953 cm^{-1} [27]. CH_3 bending deformation behavior is observed at ~1377 cm^{-1} and CH_2 bending band behavior at ~1463 cm^{-1}. The CH_2 stretching bonds are observed at ~2853, 2924 and 2953 cm^{-1}. The presence of a peak at ~1712 cm^{-1} is a proof of capping of CdSe NPs by methanol [28]. Almost all existed peaks in FTIR spectra show a slight shift behavior toward larger wavenumber as the laser fluence increases due to increase of particle size of CdSe. Finally, the FT-IR spectra revealed that the intensity of transmittance bands decreases slightly with increasing the laser fluence.

CONCLUSION

We have synthesised and investigated suspensions of CdSe nanoparticles in methanol by laser ablation. Our investigations revealed that the laser fluence causes distinctive changes in the structural, optical, morphological, and electrical properties of CdSe nanoparticles. The produced CdSe NPs in this experiment conditions have spherical shape. The average particle size of CdSe increases as laser fluence increase. A blue shift of 0.55 eV was noticed for CdSe nanoparticles prepared at lower laser fluence. All the synthesized CdSe nanoparticles possess polycrystalline hexagonal (Wurtzite) structure and small shift in peaks was observed when increasing the laser fluence. The FTIR investigation showed that the Cd–Se stretching band was observed at about 722 cm^{-1}. The sharp peak at 1000 nm is belonging to vibration band of CO. From TEM analysis, it has been observed that the synthesized CdSe nanoparticles have spherical shape with Gaussian size distribution. Photoluminescence of laser ablated CdSe particles was observed and it was noticed that the peak emitted wavelength shifted toward long wavelength as laser fluence increase.

REFERENCES

1. Ruth, A., John, A., Young, *Colloids and Surfaces A: Physicochem. Eng. Aspects*. 2006, vol. 279 P. 121.
2. Xiaocheng, Y., Chunchuan, X., Giles N.C., *J. Appl. Phys*. 2008, vol. 104, p. 073727.
3. Rathors, D., Saxena, N., Sharma K., *Chalcogenide Letters*. 2008, vol. 5, p. 21.
4. Hankare, P., Bhuse, V., Garadkar, K.M., Delekar S., Mulla I., *Semicond. Sci. Technol*. 2004, vol. 19, p. 70.
5. Murali, K., Swaminathan, V., Trivedi, D., *Sol. Energy Mater. Sol. Cells*. 2004, vol. 81, p. 113.
6. Choi, J., Kim, J.B. Yoo, Kim, D., *Sol. Energy*. 1998. V. 6, p. 41.
7. Gorer, S., Hodes, G., *J. Phys. Chem*. 1994, vol. 98, p. 5338.
8. Nair, M.T., Nair, P., Zingaro, R., Moyers, E., *J. Appl. Phys*. 1993, vol. 7, p. 1879.
9. Ramaiah, K.Y., Chang, Su, Juang, S.F., Ohdaira, K., Shiraki, Y., Liu, H.I., Chen, A., Bhatnagar, *J. Cryst. Growth*. 2001, vol. 224, p. 74.
10. Rashwan, S.M., Abdul-Wahab, S., Mohammed, M., *Mater J., Sci. Mater. Electron*. 2007, vol. 18, p. 575 .
11. Melelera, Yu., Redy Chev, N., Nevikor, G., *Inorg. Mater*. 2007, vol. 43, p. 455.
12. Semaltianos, N., Logothetidis, S., Perrie, W., Romani, S., Potter, R., Sharp, M., French, P., Dearden, G., Watkins, K., *Europhysics letters*. 2008, vol. 84, p. 47001.
13. Semaltianos, N., Logothetidis, S., Perrie, W., Romani, S., Potter, R.J., Sharp, M., French, P., Dearden, G., Watkins, K., *Applied Physics A*. 2006, vol. 94, p. 641.
14. Horoz, S., Lu, L., Dai, Q., Chen, J., Yakami, B., Pikal, J., Wang, W., Tang, *J., Applied Physics Letters*. 2012, vol. 101, p. 223902.
15. Naji, A., Habubi, N.F., Ismail, R.A., *Journal of Materials Science: Materials in Electronics*. 2014, vol. 25, p. 3190.
16. JCPDS, International center for differaction data. 1998. USA card No. 77-2307.
17. Scherrer, P., *Göttinger Nachrichten Gesell*. 1918, vol. 2, p. 98.
18. Williamson, G., Smallman R.C., *Phil. Mag*. 1959, vol. 1, p. 34.
19. Epifani, M., Giannini, C., Manna, L., *Materials Letters*. 2004, vol. 58, p. 2429.
20. Ismail, R.A., *Micro & Nano Letter*. 2011, vol. 6, p. 951.

21. Gudage, Y., Deshpande, N., Sharma, R., *J. Phys. Chem. Solids*. 2009, vol. 70, p. 907.
22. Somma, F., Nikl, M., Nitsch, K., Giampaolo, C., Phani, A., Santucci, S., *Superficies y Vacío*. 1999, vol. 9, p. 62.
23. Ismail, R., Ali, A., Ismail, M., Hassoon, K., *Applied Nanoscience*. 2011, vol. 1, p. 45.
24. Beard, M., Turner, G., Schmuttenmaer, C., *Nano Lett*. 2006, vol. 9, p. 983.
25. Yakuphanoglu, F., Cukurovali, A., Yilmaz, I., *Optical Materials*. 2005, vol. 27, p. 1363.
26. Mahajan, S., Rani, M., Dubey, R., Mahajan, J., *International journal of Latest Research in Science and Technology*. 2013, vol. 2, p. 457.
27. Hamizi, N., Shiau, C., Johan, M., *Int. J. Electrochem. Sci*. 2012, vol. 7, p. 4727.
28. Hamizi, N., Shiau, C., Johan, M., *J. Mat. Chem. Phys*. 2010, vol. 124, p. 395.